Control Architecture for Segmented Trajectory Following of a Wind-Propelled Autonomous Catamaran

Gabriel H. Elkaim and Robert J. Kelbley

University of California, Santa Cruz, Santa Cruz, CA, 95064, USA

Abstract

An autonomous surface vehicle, based on a Prindle-19 catamaran and substituting a self-trimming vertical wing for the sail, was developed to demonstrate precision guidance and control. This vehicle, the Atlantis, was demonstrated to track straight line segments to better than 0.3 meters (one σ) when already trimmed for sail along the segment. In order to make the Atlantis useful as an autonomous vehicle, however, more complicated paths are required than simple straight line segments. A segmented trajectory is developed based on waypoints, segments, and arcs as the path primitives. A control architecture is also developed which can traverse a segmented trajectory made of linked path primitives, given reachability constraints due to wind direction. For segments where the destination is unreachable due to the wind direction a lane width is established and an on-the-fly tacking mode is used to traverse the segment while remaining within the lane width. A nonlinear model of the catamaran was simulated using Simulink, including realistic wind and current models. The control architecture was applied to the simulated catamaran using Monte Carlo simulations which demonstrated very robust segment traversal while maintaining a crosstrack error of less than one meter throughout the path.

I. Introduction

Autonomous marine navigation using wind-powered propulsion has been demonstrated by the Atlantis to an accuracy better than 0.3 meters (one σ) for line following applications. This achievement hints at the possibilities of autonomous ocean vehicles which can traverse great distances restricted only by the availability of wind and electronic positioning systems. Wind-propelled

Assistant Professor, Department of Computer Engineering, UCSC, 1156 High St., Santa Cruz, CA, 95064, USA.

Graduate Student, Department of Computer Engineering, UCSC, 1156 High St., Santa Cruz, CA, 95064, USA.

Autonomous Surface Vehicles (ASV's) can provide unmanned coastal cruising capabilities with energy efficiency for a myriad of sensing and scientific measurement missions.

The addition of a more advanced guidance system using waypoint navigation to the Atlantis will allow it to perform as a fully functional ASV. The control architecture for this guidance system uses a fixed series of latitude and longitude coordinates to mark points along the way to its final destination. The details of the control architecture for this segmented trajectory following model will be outlined, including details of the simulation models used throughout testing.

The key components of the Atlantis are discussed in Section II, including previous results of precise line following control. The different simulation models used for guidance system testing are shown in Section III including the nonlinear model of the ocean vehicle, water current and wave disturbances, and the wingsail propulsion system. An analysis of the closed loop controller used is highlighted in Section IV. The generation of segmented trajectories consisting of arcs and lines to connect waypoints is then outlined in Section V, including a real-time tacking procedure to traverse line segments that are unreachable due to wind direction limitations. The nonlinear 3 DOF (Degrees of Freedom) simulation results are presented in Section VI and finally a conclusion is provided in Section VII.

Fig. 1.   Atlantis with wingsail, January 2001.

II. The Atlantis

A. System Overview

The Atlantis, pictured in figure 1, is an unmanned, autonomous, GPS-guided, wingsailed sailboat. The Atlantis has demonstrated an advance in control precision of a wind-propelled marine vehicle to an accuracy of better than one meter. This quantitative improvement enables new applications, including unmanned station-keeping for navigation or communication purposes, autonomous "dock-to-dock" transportation capabilities, emergency "return unmanned" functions, precision marine science monitoring [8], and many others still to be developed. The prototype is based on a modified Prindle-19 light catamaran.

The wind-propulsion system is a rigid wingsail mounted vertically on bearings to allow free rotation in azimuth about a stub-mast. Aerodynamic torque about the stub-mast is trimmed using a flying tail mounted on booms joined to the wing. This arrangement allows the wingsail to automatically attain the optimum angle to the wind, and weather vane into gusts without inducing large heeling moments. Modern airfoil design allows for an increased lift to drag ratio (L/D) over a conventional sail, thus providing thrust while reducing the overturning moment.

The system architecture is based on distributed sensing and actuation, with a high-speed digital serial bus connecting the various modules together. Sensors are sampled at 100Hz., and a central guidance navigation and control (GNC) computer performs the estimation and control tasks at 5Hz. This bandwidth has been demonstrated to be capable of precise control of the catamaran.

The sensor system uses differential GPS (DGPS) for position and velocity measurements, augmented by a low-cost attitude system based on accelerometer- and magnetometer-triads. Accurate attitude and determination is required to create a synthetic position sensor that is located at the center-of-gravity (CG) of the boat, rather than at the GPS antenna location.

Previous experimental trials recorded sensor and actuator data intended to excite all system modes. A system model was assembled using Observer/Kalman System Identification (OKID) techniques [5]. An LQG controller was designed using the OKID model, using an estimator based on the observed noise statistics. Experimental tests were run to sail on a precise track through the water, in the presence of currents, wind, and waves.

B. Previous Line Following Control Results

In order to validate the performance of the controllers and all up system, closed loop control experiments were performed in Redwood City Harbor, California, on January 27, 2001. These tests were intended to verify that the closed loop controllers were capable of precise line following with the increased disturbances due to the wingsail propulsion. No modifications were made to the LQR controller design, and the tests were run on a day with approximately 12 knots (or 6 m/s) of wind, with

gusts up to the 20 knot (or 10 m/s) range.

Upon analyzing the data, it was demonstrated that the Atlantis was capable of sailing to within 25 degrees of the true wind direction. Figure 2 presents a close-up of the first path of regulated control, and looks at the crosstrack error, azimuth error, and velocities while tracking a line. Note that the dark line in the top of the boat speed graph is the wind speed, and can be seen to vary well over 50% of nominal.
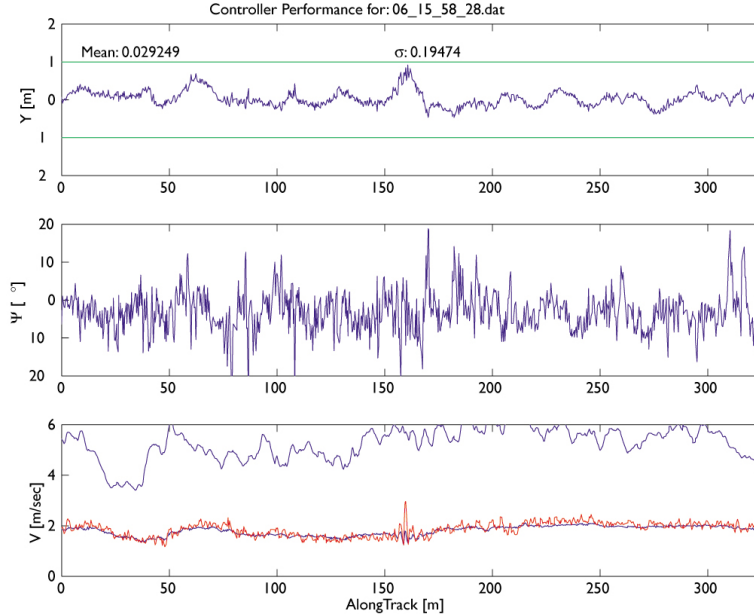

Fig. 2. Sailing path errors.

The mean of the crosstrack error is less than 3 cm., and the standard deviation is less than 30 cm., note that this is the Sailboat Technical Error (STE, the sailing analog of Flight Technical Error) defined as the difference between the position estimated by the GNC computer and the desired sailboat position. Previous characterization of the coast-guard differential GPS receiver indicated that the Navigation Sensor Error (NSE) is approximately 36 cm., thus the Total System Error (TSE) is less than 1 meter.

III. SYSTEM MODELS

A. Vehicle Model

In order to simulate control of the Atlantis a nonlinear 3 DOF system model was needed. While several good modeling techniques exist to model a powered boat through the water [3], they remain complicated and difficult to calculate. To formulate the equations of motion, the Atlantis is assumed to be travelling upon a straight line, conveniently assumed to be coincident with the X-axis, through the water at a constant speed, V_x. The distance along that line is referred to as X, the along-track distance. The perpendicular distance to the line is referred to as Y, the crosstrack error, and the angle that the centerline of

the Atlantis makes with respect to the desired path is defined as Ψ, the angular error. This frame is referred to as the *control frame*. Figure 3 illustrates the mathematical model of the assumed path of the Atlantis, where Y, Ψ, and δ are defined as the crosstrack error, azimuth error, and rudder angle, and L is the length from the center of gravity (CG) of the boat to the center of pressure of the rudders.
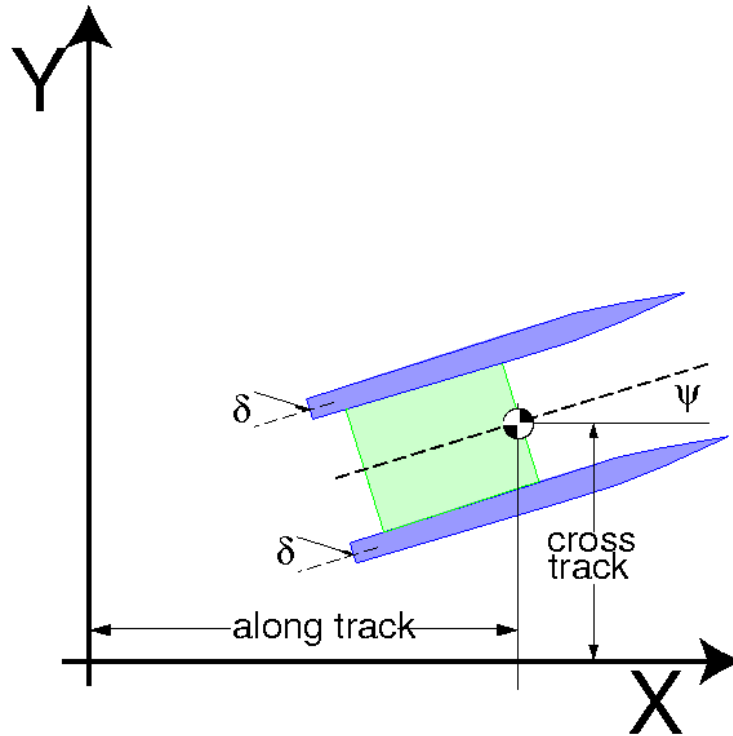

Fig. 3. Control frame definitions.

These simplified equations of motion are insufficient to model the boat to great precision, but are an excellent basis for simulating controlled trajectory following for the catamaran.

This model is a simple kinematic model that assumes that the rudders cannot move sideways through the water; that is this model places a kinematic constraint upon the motion of the entire boat. In order to simplify the equations of motion, these equations are written in the *body frame*, which is rigidly attached to the vehicle having the x-axis pointing directly from the bow of the boat and y-axis pointing out the starboard side. In these coordinates, the equations of motion are:

$$\dot{x} = V_x \tag{1}$$

$$\dot{y} = 0 \tag{2}$$

$$\dot{\Psi} = \frac{V_x}{L} \sin(\delta) \tag{3}$$

Based on prior data, though simplified, a kinematic model yields good experimental results. Using steady state turn data, we computed an effective length for the centerboard to rudder distance, L, which was found to be 2.95 m. Figure 4 shows the experimental constant turning radius data used for centerboard to rudder distance calculations.
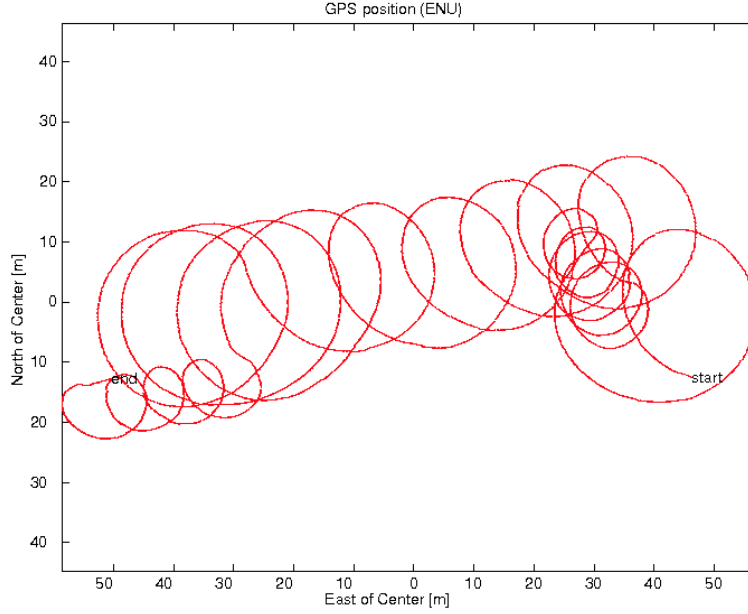

Fig. 4.   Trajectory of Atlantis as viewed from above when generating turning radius data at constant rudder angles.

The North-East-Down (NED) coordinate system attached to the Earth is used as the *navigation frame*. The relative orientation of the body frame to the navigation frame is described using the [3-2-1] Euler angles: yaw (ψ), pitch (θ), and roll (ϕ). In this work, the full vehicle 6 DOF model is reduced to 3 DOF by assuming the vehicle will remain level on the water surface (and hence that the pitch and roll angles are very small).

The desired heading of the Atlantis in the navigation frame is the trajectory generated from the control architecture discussed in Section V and will be defined as Ψ_{ref}. Therefore, knowing the heading error from the control frame (Ψ) and the control frame's orientation to the navigation frame (Ψ_{ref}), the body frame parameters can be transformed to the navigation frame where Ψ_{boat} is the orientation of the body frame in the navigation frame (the heading of the boat in reference to North):

$$\Psi_{boat} = \Psi_{ref} + \Psi \tag{4}$$

$$\dot{N} = V_x \cos\left(\Psi_{boat}\right) \tag{5}$$

$$\dot{E} = V_x \sin\left(\Psi_{boat}\right) \tag{6}$$

B. Water Current and Wave Disturbance Model

A combination of two Gauss-Markov processes were used to model water currents and wave disturbances on the surface craft. That is, the disturbances are modelled as:

$$\dot{V}_{current} = \frac{-1}{\tau_{current}} V_{current} + \nu_{current} \tag{7}$$

$$\dot{V}_{wave} = \frac{-1}{\tau_{wave}} V_{wave} + \nu_{wave} \tag{8}$$

$$V_{dist} = V_{current} + V_{wave} \tag{9}$$

Where τ is a time constant, and ν is white noise. These are tuned to match experimental data by changing the correlation time constant and the standard deviation of the white noise. The first Gauss-Markov process is assumed to be water currents that change gradually over time. The second process models waves that produce higher frequency disturbances on the boat's hull. An exact analog formula is used for the direction of the waves (and also the wind).

These disturbances are assumed to alter the velocity of the boat in the navigation frame (Eq. 5-6) directly:

$$\Psi_{boat} = \Psi_{ref} + \Psi \tag{10}$$

$$\dot{N} = V_x \cos\left(\Psi_{boat}\right) + V_{dist} \cos\left(\Psi_{dist}\right) \tag{11}$$

$$\dot{E} = V_x \sin\left(\Psi_{boat}\right) + V_{dist} \sin\left(\Psi_{dist}\right) \tag{12}$$

Figure 5 shows a water speed and direction model generated from the combination of these stochastic processes.

C. Wingsail Propulsion Model

The wingsail propulsion system works like a conventional sail, which generates force from the wind to produce the boat's speed, V_x. Like all traditional sailboats, the maximum boat speed is a function of the relative angle between the boat and the wind. While the wingsail does not suffer from aeroelastic collapse (and can thus point higher into the wind), it still cannot generate forces that will propel the boat directly upwind.

The wind speed and direction are based on a first order Gauss-Markov stochastic process identical to those producing the current and wave disturbances described in Eq. 9.

Wing lift (L) and drag (D) forces were derived using simplified Glauert lifting line theory [7], [9], with the drag assumed to be entirely induced drag. Thus, the wing lift is modeled as:
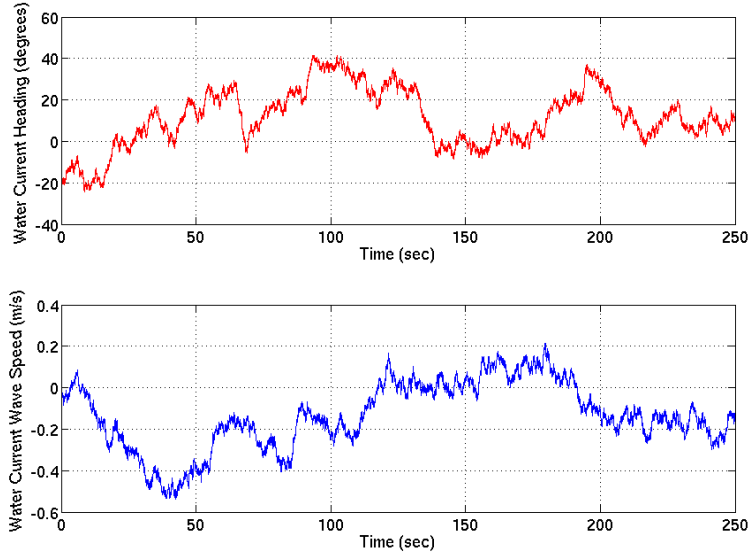
Fig. 5.   Sample water current and wave disturbance models.

$$L = \frac{1}{2}\rho S C_L |V|^2 \tag{13}$$

$$D = \frac{1}{2}\rho S C_D |V|^2 \tag{14}$$

where ρ is the density of the medium, V is the velocity through the medium, S is the surface area of the wing, and C_L is the lift coefficient and C_D is the drag coefficient.

To calculate the maximum boat speed for each relative wind angle, the boat is assumed to be at a constant velocity requiring all forces on the boat to be in balance. The longitudinal components (or body x-axis components) of all of the forces, with the addition of hull flat plate drag are summed to zero, and thus the maximum speed V_{max} can be found.

$$\sum F^x = L^x_{wing} + D^x_{wing} + D_{hull} = 0 \tag{15}$$

Using previous experimental wind and boat velocity information, the product of the hull effective surface area and drag coefficient was found ($S_{hull}C_{D_{hull}}$). The solution to this quartic equation, Eq. 18, for the speed ratio vs. heading is plotted in polar coordinates in figure 6.

$$K = \left(\frac{\rho_{H_20} S_{hull} C_{D_{hull}}}{\rho_{air} S_{wing} C_{L_{wing}}} \right)^2 \tag{16}$$

$$\sigma = \sin\left(\Psi\right) - (D/L)\cos\left(\Psi\right) \tag{17}$$

$$\left((D/L)^2 - K\right)V_{max}^4 + 2V_{wind}(D/L)\left((D/L)\cos(\Psi) - \sigma\right)V_{max}^3$$

$$+ V_{wind}^2 \left((D/L)^2 + \sigma^2 - 4(D/L)\sigma\cos(\Psi)\right)V_{max}^2$$

$$+ 2V_{wind}^3\sigma\left(\sigma\cos(\Psi) - (D/L)\right)V_{max} + V_{wind}^4\sigma^2 = 0 \tag{18}$$

where in Eq. 18 $\Psi = \Psi_{boat} - \Psi_{wind}$.
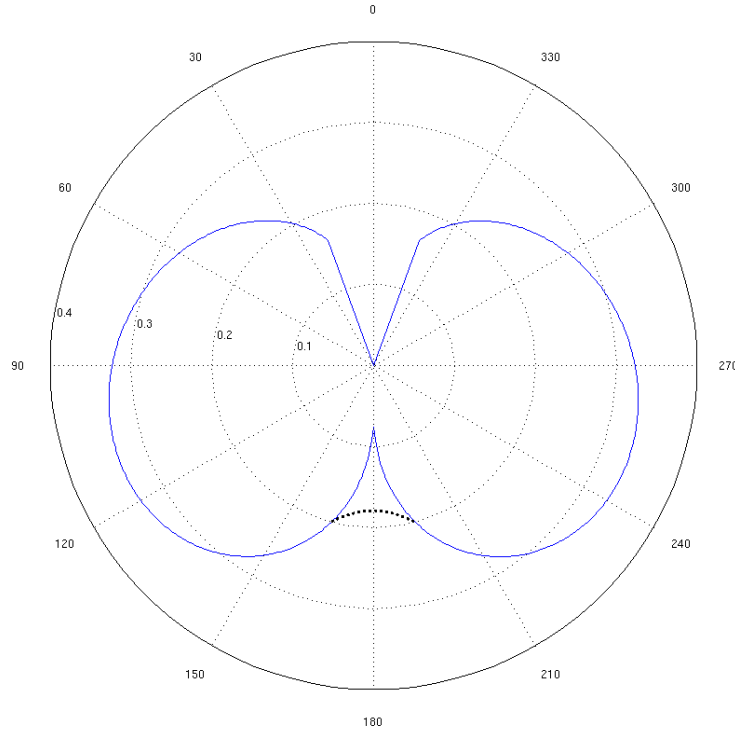
Fig. 6.   Wind Angle vs $\frac{|V_{max}|}{|V_{wind}-V_{max}|}$.

When running downwind the propulsion is based mainly on drag, as opposed to lift. In this case the simplified analysis fails to take into consideration the additional drag from a stalled wing. To account for this added propulsion a spline has been inserted into the speed ratio plot to more accurately represent boat speed when the Atlantis is running before the wind.

Lastly, in order to simulate the momentum of the Atlantis through the water, the speed is low-pass filtered, with a time constant of approximately 5 seconds. This provides a response comparable to experimental results without needing to estimate either the exact mass nor the complicated hull water interactions.

$$V_x(s) = \frac{0.2}{s + 0.2} V_{max}(s) \tag{19}$$

IV. CONTROLLER ANALYSIS

A simple proportional plus integral (PI) feedback controller is used to stabilize the nonlinear boat model when following trajectories in the presence of wave disturbances. The controller takes as input the boat's heading error (Ψ_{error}) and crosstrack error (Y_{error}). Proportional and integral gains are then applied to these inputs to generate a reference rudder angle (δ_{ref}) to direct the boat back on its proper trajectory.

It was previously shown [1] that our boat model will loose stability as the boat speed reaches a certain point beyond the controller's design point V_x^{design}. To address this problem, the controller can compensate for the boat's speed using a gain-scheduled controller or by applying input pre-scaling to obtain a velocity invariant controller. In our simplified model, we will instead show that our controller is stable up to a specific boat speed point, which can never be exceeded in any of our simulations.

The boat speed design point $V_x^{design} = 2.0$ m/s was used to find controller gain values that minimized steady state errors in the presence wave disturbances and provided a quick transient response. The Eqs. 3-6 were then linearized around a small variance in boat heading providing the linearized equations:

$$\dot{\Psi} = \frac{V_x}{L}\delta \tag{20}$$

$$\dot{N} = V_x \tag{21}$$

$$\dot{E} = V_x \Psi_{boat} \tag{22}$$

A block diagram of the linearized equations combined with the closed loop PI controller gains is shown in figure 7. Assuming the reference heading for the boat is due North ($\Psi_{ref} = 0°$), the transfer function for the closed loop system is then formulated as:

$$Y_{error}(s) = \left(\frac{V_x^2}{L}\right) \frac{s}{s^3 + \frac{K_\Psi V_x}{L}s^2 + \frac{K_Y V_x^2}{L}s + \frac{K_{Y_i} V_x^2}{L}} \tag{23}$$

where for our controller design $K_Y = 3.0$, $K_{Y_i} = 0.25$, and $K_\Psi = 2.0$.

A mapping of the closed loop system poles from Eq. 23 is shown in figure 8 as a function of V_x. The closed loop system
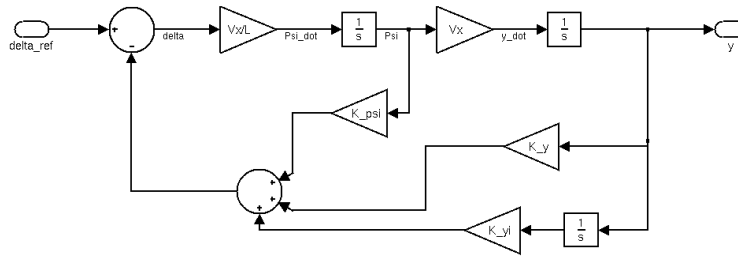
Fig. 7. Block diagram of linearized boat equations combined with PI controller gains.

poles will remain stable as the boat's speed is increased for this linearization of our kinematic equations. The natural frequency of the linearized closed loop system for $V_x^{design} = 2.0$ m/s is 2.0 rad/s. Testing of the nonlinear model was then performed by simulating a step input for the crosstrack and heading errors and observing the resulting steady state system response. A stable response was observed for boat velocities up to 7 m/s, well beyond the maximum operating point for the wing-sail propulsion system.
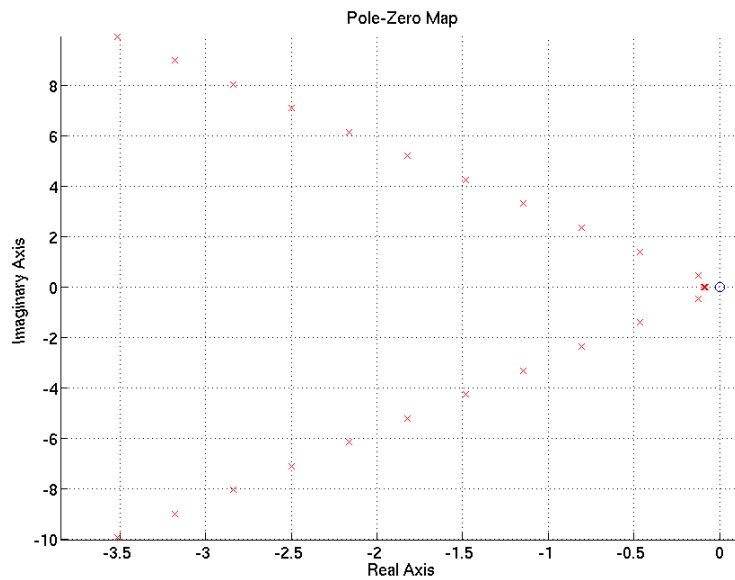

Fig. 8. Mapping of closed loop system pole locations as a function of increasing boat speed.

V. Segmented Trajectory Generation

A. Arcs and Lines

The waypoint navigation system uses a series of user defined waypoints as reference points for navigation. The Atlantis could simply use these waypoints as heading references, however large crosstrack errors would be produced during waypoint transitions and certain references may be unreachable because of the wind direction. A segmented trajectory of lines connected by arcs of a constant radius is used to provide a path of achievable trajectories.

Arc segments are added between line segments such that the line segments are tangent to the arc where they meet. Figure 9 demonstrates how waypoint inputs are transformed to line and arc segments. In practice, segments will be created in real-time as waypoints are achieved allowing for tacking scenarios to be applied when necessary.
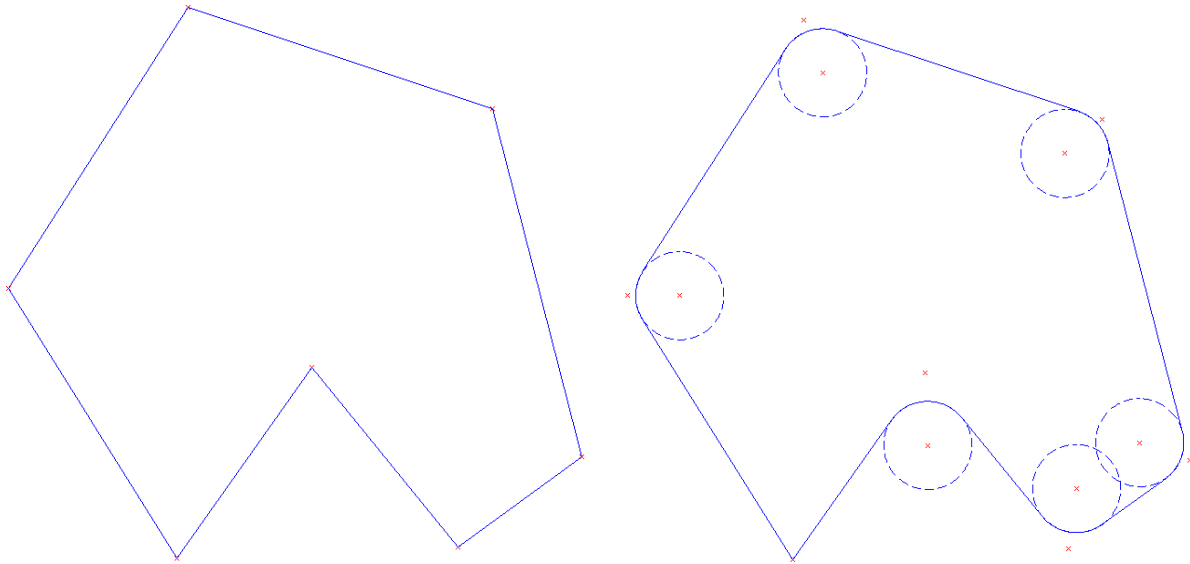

Fig. 9.   User defined waypoints (left) transformed into arc and line segments (right).

B. Tacking Algorithm

In sailing, a tack is performed when the boat turns such that the bow passes through the wind. Tacking (as a sailing procedure) then refers to the process of making alternate tacks as close as possible to the wind, allowing a sailboat to effectively sail upwind. As shown in figure 6, if the Atlantis attempts to sail directly upwind it will eventually be "in irons" meaning it will lose all speed and stall out. A *lane width* for the desired line segment is defined and used to tack back and forth through the desired heading until the next waypoint is reached. The Atlantis must be prepared to tack at any point should the wind change and the waypoint become unreachable. As such, a real-time tacking algorithm was developed for the guidance system that provides navigation within the defined lane width allowing waypoints to be achieved while avoiding unreachable points of sail.

Figure 10 depicts an ocean vehicle traversing a line segment with a varying wind direction (left side). As the wind shifts inside a defined wind heading allowance, the water craft adjusts its heading to navigate within the desired lane width.

C. Initial Segment Acquisition

Unless the vehicle starts in the exact same position as the first line segment, a technique to provide a reference heading that progressively locks on to the first segment must be used. A reasonable heading for the vehicle would be to command the boat
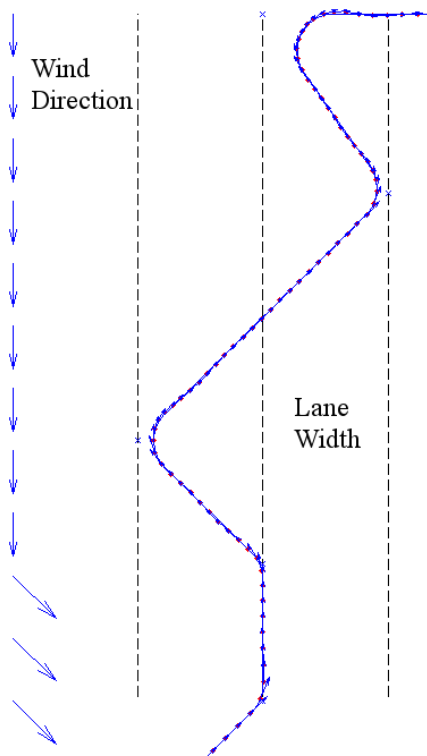
Fig. 10. Surface vehicle adjusting to tacking routine in reaction to changing wind headings (left side).

to a $90°$ angle towards the line until it gets closer, and then angle towards the line in the direction of the desired navigation.

An easy method to achieve this curved trajectory is to create a reference heading to the line that is a function of the vehicle's crosstrack in the control frame. By definition, as the surface craft moves closer to the desired line segment, its crosstrack will approach zero. Therefore, a desired heading to the line can be derived as:

$$\Psi_{ref}^{control} = \arctan\left(\frac{Y}{\tau}\right) \tag{24}$$

where Y is the crosstrack value and τ is a constant that determines how steep a trajectory the boat will take to acquire the line. Figure 11 shows the Atlantis using this technique for line acquisition using $\tau = 5$ and then switching to the PI controller for line following when $Y < 0.5\ m$.

VI. SIMULATION RESULTS

Using the boat, wind, and wave models outlined in Section III, the PI controller discussed in Section IV was used to follow the set of trajectories generated from predefined waypoints as described in Section V. The controller monitors both the heading error Ψ and crosstrack Y to adjust the rudder position δ. First, a surface vehicle propelled by a constant speed source such as an outboard motor is simulated. Figure 12 shows the resulting path and figure 13 displays the heading error and crosstrack
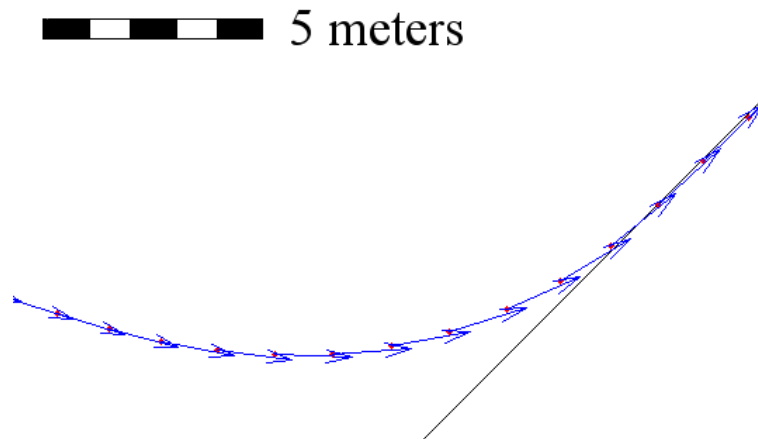
Fig. 11. Acquisition of first segment from distant initial vehicle position.

error for such a boat. Monte Carlo simulations providing different random values for wind and wave disturbances show the boat to have an average heading error of 2.2^o and an average crosstrack error of 2 cm. as shown in Table I.

	Motorboat			Sailboat		
	Lines	Arcs	Total	Lines	Arcs	Total
$\Psi_{avg}(^o)$	0.69	10.9	2.20	1.20	11.7	3.25
$\Psi_{\sigma}(^o)$	4.85	18.6	9.42	8.99	17.8	12.6
$\Psi_{max}(^o)$	18.3	34.8	34.8	53.9	40.1	63.0
$Y_{avg}(m)$	0.01	0.15	0.02	0.01	0.27	0.06
$Y_{\sigma}(m)$	0.08	0.30	0.16	0.10	0.45	0.28
$Y_{max}(m)$	0.42	0.82	0.82	0.47	1.22	1.23

TABLE I

SIMULATION RESULTS.

Using the same PI controller, the varying wingsail speed model was used with the tacking algorithm to follow the same set of waypoints with identical disturbances. The vehicle path and average wind direction is displayed in figure 14 and resulting heading error and crosstrack error information is shown in figure 15. As with the motorboat, Monte Carlo simulations were completed showing the Atlantis to have a simulated average heading error of 3.25^o and an average crosstrack error of 6 cm. Sailboat results are also shown in Table I.

VII. CONCLUSIONS

A control architecture for an autonomous sailboat using a waypoint navigation system and simulated with a PI controller is capable of providing robust and reliable guidance under realistic wind and water disturbance models. This architecture was applied to a simplified model of the Atlantis, a wingsail propelled catamaran previously shown capable of line following accuracy better than 0.3 meters. Simulations modeling similar experimental conditions previously encountered show that precision control is possible for waypoint navigation requiring segmented trajectory following of arcs and lines and real-time waypoint
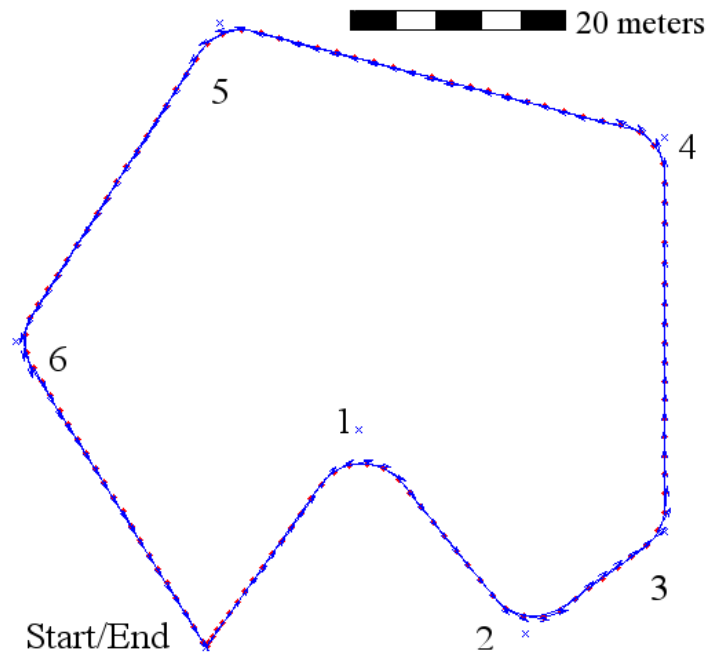
Fig. 12. Control architecture applied to surface vehicle simulated with constant speed propulsion with water current and wave disturbances.
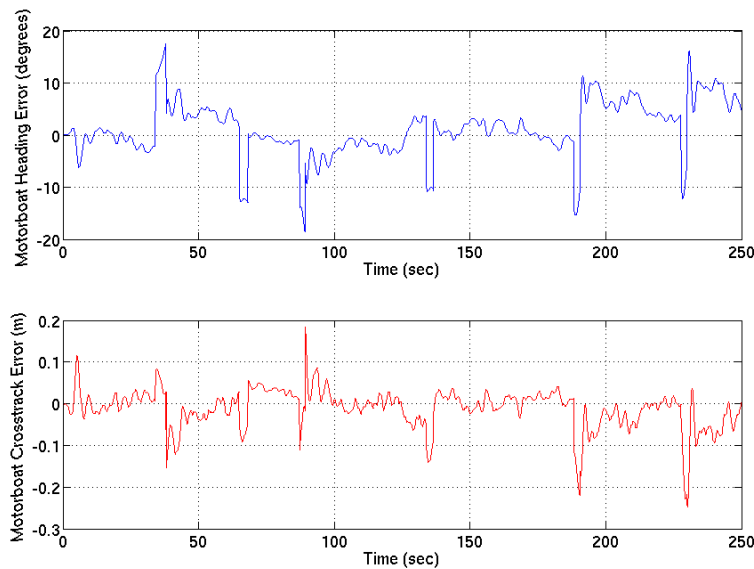

Fig. 13. Heading and crosstrack error for constant speed surface vehicle simulation

management to prevent unreachable points of sail. Simulations show the sailboat can be controlled to better than one meter accuracy.

This control architecture is not limited to PI controllers, and more advanced controllers will presumably allow for better system accuracy. The simulation environment discussed will also serve as a development platform for controller comparisons and Hardware-in-the-Loop testing of the ship's sensors, actuators, and complete GNC system.

Future work will include a waypoint generation methodology that will avoid stationary obstacles and also optimally determine trajectories given only a destination point and weather data forecasts to predict future wind activity. This added guidance system
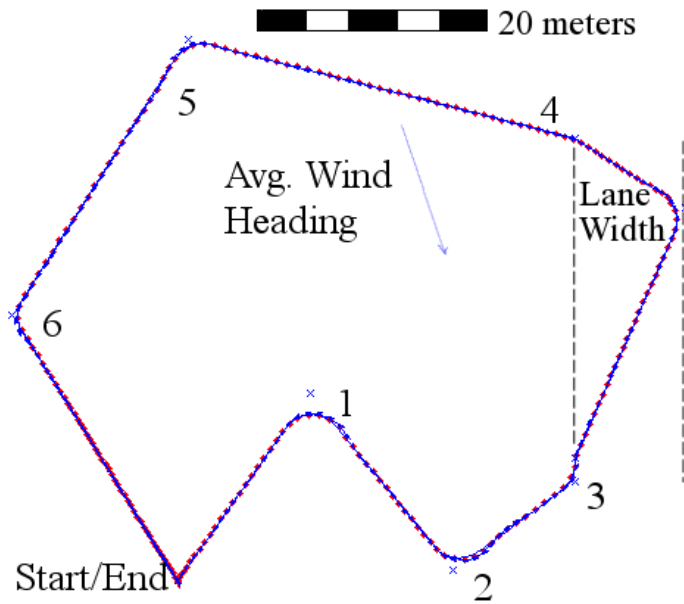
Fig. 14.   Control architecture applied to wingsailed vehicle simulated with water current and wave disturbances.
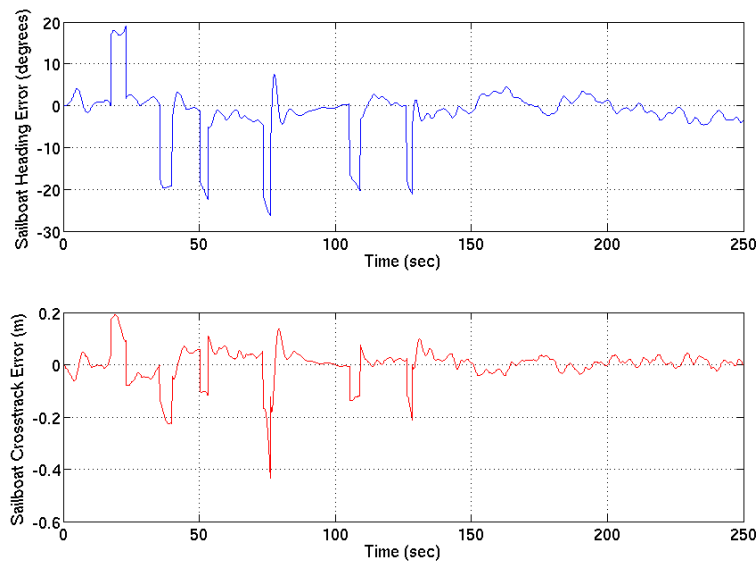

Fig. 15.   Heading and crosstrack error for wingsailed surface vehicle simulation.

combined with advancements in Atlantis sensors and actuators will create a wind-propelled ASV capable of robust navigation

that can be used for a variety of future marine applications.

REFERENCES

[1] G.H. Elkaim. *System Identification for Precision Control of a Wingsailed GPS-Guided Catamarn*. PhD thesis, Stanford University, 2001.

[2] P. Encarnacao, A. Pascoal, and M. Arcak. Path following for autonomous marine craft. *5th IFAC Conference on Maneuvering and Control of Marine Craft*, pages 117–22, 2000.

[3] T. Fossen. A nonlinear unified state-space model for ship maneuvering and control in a seaway. *Intl Journal of Bifurcation and Chaos*, 15:2717–2746, 2005.

[4] T.I. Fossen. *Guidance and Control of Ocean Vehicles*. Wiley and Sons, New York, NY, 1994.

[5] J.-N. Juang. *Applied System Identification*. Prentice Hall, NJ, 1994.

[6] E. Lefeber, KY. Pettersen, and H. Nijmeijer. Tracking control of an underactuated ship. *IEEE Transactions on Control Systems Technology*, 3:52–61, 2003.

[7] B.W. McCormick. *Aerodynamics, Aeronautics, and Flight Mechanics*. John Wiley and Sons, New York, NY, 1979.

[8] A. Pascoal, P. Olivera, and C. Silvestre. Robotic ocean vehicles for marine science applications: The european asimov project. *OCEANS 2000 MTS/IEEE Conference and Exhibition*, 1:409–415, 2000.

[9] R.S.Shevell. *Fundamentals of Flight*. Prentice-Hall, Inc., Englewood Cliffs, NJ, 1983.

[10] R. Skjetne and T. Fossen. Nonlinear maneuvering and control of ships. *MTS/IEEE OCEANS 2001*, 3:1808–15, 2001.

[11] T. VanZwieten. *Dynamic Simulation and Control of an Autonomous Surface Vehicle*. PhD thesis, Florida Atlantic University, 2003.